Scaled Total Hemispherical Emittance of Particle-Gas Layers

HaeOk Lee*
University of Minnesota, Minneapolis, Minnesota

A radiation scaling technique is applied to problems with scattering particles and spectrally selective gases. A solution method, which uses a combination of the scaling and the exponential wideband modeling, is developed. The solution procedure is used to obtain the hemispherical emittance of isothermal layers, composed of absorbing gas of H_2O or CO_2, together with isotropically scattering particles. The scaled equivalent results are compared to calculations available from the path length distribution solution. Excellent comparisons are obtained for low to moderate absorbing gas pressures and for low to moderate particle optical depths and albedo. Suggestions to improve the accuracy of the scaled solution for large or scattering dominant problems are also included.

Nomenclature

a = absorption coefficient
A_j = wideband gas absorption for band j
A_1, A_2 = surface area of top or bottom reflecting wall, respectively
$\langle\cos\theta\rangle$ = scattering phase function asymmetry factor
e_{bb} = blackbody emissive power
E_{p-g} = hemispherical total emittance of particle-gas layer
E_3 = exponentiaal integral function of order 3
$f(\nu T)$ = blackbody fraction
$F_{1\text{-}2}$ = configuration factor from surface 1 to 2
k = extinction coefficient
L = thickness of the emitting layer
$P(\cos\Theta)$ = scattering phase function
P_a = partial pressure of the absorbing gas species
$q^-\nu(0)$ = outward spectral radiative heat flux of the layer at position $\kappa = 0$
S = variable path length
T = temperature of the emitting layer
y = coordinate direction
X = Mie particle size parameter
α_b = integrated band intensity
$\langle\alpha\rangle$ = total geometric-mean absorptance
γ = relative gas absorption ($a_{g\nu}/k_p$)
η_b = pressure broadening parameter
θ = polar angle measured from the normal direction y
Θ = angle between the incident and the scattering directions
κ = optical depth ($k \cdot y$)
κ_H = optical depth at gas bandhead or center
κ_L = total optical depth of layer thickness L
μ = $\cos\theta$
ρ_E = equivalent wall reflectivity
σ = scattering coefficient or the Stefan-Boltzmann constant
$\tau_\nu(S)$ = transmittance (e^{-kS})
$\langle\tau\rangle$ = total geometric-mean transmittance
ω = scattering albedo
ω_b = exponential band decay width

Superscripts

$*$ = dimensionless quantity
$-$ = into the negative y direction

Subscripts

a = anisotropic scattering
b = band quantity
E = equivalent nonscattering
g = gas quantity
i = isotropic scattering
j = at gas band j
l = lower band limit
p = particle quantity
ν = spectral or wave number dependent
u = upper band limit

Introduction

THE layers under study are isothermal, plane parallel, one-dimensional slabs that absorb, emit, and scatter thermal radiation. They are composed of homogeneous suspensions of small particles in a radiatively participating gas. Such layers are idealizations of mixtures that might result from a combustion process or fluids that have been intentionally seeded to enhance the heat transfer characteristics. The radiative heat transfer from a layer at high temperatures can be characterized by the total hemispherical emittance, which is a direction- and wave number-averaged comparison of the layer's emission, to the blackbody emission at the same temperature. Within a layer, the mechanism for radiative transfer is complex and modeling the transfer can be a formidable task even for a simple geometry. Two factors combine to add to the complexity of the calculation: the highly spectral or nongray nature of molecular gas absorption and the anisotropic scattering by the particles. The goal of this study is to find a simple, yet accurate, solution technique that can be used to model these complex phenomena.

There are two radiation heat transfer calculation procedures for particle-gas mixtures: the path length distribution method and the exponential series method.[1] The path length distributions are the probabilities that the photons with particular travel lengths within a pure scattering layer will contribute to the type of energy transfer in question, e.g., transmission or reflection. Particle and gas absorptions act to exponentially lessen the strength of the photon contributions. A study of the total hemispherical emittance of an isothermal layer composed of isotropically scattering particles and absorbing gases has

Presented as Paper 87-1486 at the AIAA 22nd Thermophysics Conference, Honolulu, HI, June 8-10, 1987; received Aug. 31, 1987; revision received Nov. 23, 1987.

*Assistant Professor, Department of Mechanical Engineering. Member AIAA.

been presented by Skocypec and Buckius.[2] The second calculation method is the exponential series method where the gas absorptance is fit with an exponential series. The resulting empirical absorption coefficient is used to solve the equation of transfer, including the scattering, at each wavelength.[3] A comparison of the two techniques shows that they can be equivalent,[1] but both are computation intensive.

The solution approach of this study is to combine scaling ideas with a wideband gas model. The anisotropic scattering effects are included by applying the scaling laws already developed for one-dimensional planar layers.[4,5] The scaling proceeds in two steps to reduce an anisotropic scattering layer to a nonscattering layer. The nondimensional parameters that determine the solution of the normalized problem are transformed by the scaling laws. Good accuracy for heat transfer results have been reported with the scaling, when gray or a single wave number analysis is considered. The task here is to apply the scaling to layers where the spectral integration is important. The emittance of the scaled problem is obtained by an enclosure analysis that includes the effect of the absorbing gases.[6] The particles considered are all isotropic scatterers, although the formulation is presented for anisotropic scatterers, as well. The absorbing gases are taken to be either H_2O or CO_2. The gas spectral characteristics are same as those used in Ref. 2.

This paper is organized in the following manner. The formulation section begins with a discussion of the particle and gas properties, and their relationship to the scaling laws. The details of the emittance calculation for the scaled layer are then presented, along with a description of how the gas band absorption is included. Some comparisons between the scaled results and exact results, obtained by Skocypec et al.[8] using the photon path length approach, are presented and discussed in Results and Discussion. Summary and recommendations are contained in Conclusions.

Formulation

Scaling Properties

A scattering layer with black boundaries (reflectivity of zero) can be described by its properties: extinction coefficient k, the single scattering albedo ω, and the scattering phase function $P(\cos\Theta)$. The extinction coefficient, which characterizes the attenuation of radiation in the medium, is a sum of the absorption coefficient a and the scattering coefficient σ. The geometric depth multiplied by the extinction coefficient results in the dimensionless optical depth κ. The ω is the ratio of the scattering to extinction coefficients, and it indicates the importance of scattering for the medium. The nonuniform angular redistribution of incident radiation by the scattering component is described by the phase function P, where Θ is the angle between the incident and the scattered directions. The equivalent nonscattering layer is described with a scaled optical depth κ_E and an equivalent wall reflectivity ρ_E. Since the scaled layer only absorbs and emits radiation, ρ_E is introduced as a variable to retain the scattering characteristics of the layer.

The scattering mixture is made up of both particles and gases. Therefore, both components contribute to medium properties. The relationships between the mixture and the component properties are

$$k = k_p + k_{g\nu} = (\sigma_p + a_p) + a_{g\nu} \tag{1a}$$

$$\omega = \omega_p/(1+\gamma) \tag{1b}$$

$$\gamma = a_{g\nu}/k_p \tag{1c}$$

The subscript p refers to the particle properties, and g refers to the gas properties. Properties without an explicit p or g designation refer to the mixture properties. The scattering properties are considered to be strictly particle properties, since the molecular scattering from gases is very small compared to particle scattering. The subscript ν refers to the wave number (cm^{-1}), and its use makes the spectral dependence of a_g explicit.

The $a_{g\nu}$ is a required property for describing the mixture. For this study, the exponential wideband model is used to describe the gas absorption.[7] The model takes advantage of the banded structure of the gas absorption and uses three parameters to describe A_j, the integrated absorptance of the jth band. These parameters are the integrated band intensity α_b, the exponential band decay width ω_b, and the pressure broadening parameter η_b. A dimensionless band absorption is defined as $A_j^* = A_b/\omega_b$, and correlations for A_j^* are given as functions of η_b and κ_H, the optical depth at the bandhead or the center. The κ_H is directly proportional to the path length through the gas, while η_b, ω_b, and α_b are also functions of gas temperature. The gas absorption coefficient information is embedded in the A_j by $A_j = \int_{\nu_l}^{\nu_u} [1 - \exp(-a_{g\nu})]\, d\nu$, where the integration is over the wave number limits of the band j. Since the path length S through the layer is variable, it is difficult to know $a_{g\nu}$ explicitly. One goal of this study is to use the integrated band absorptance directly in the particle-gas emittance formulation.

The particle properties have a weak spectral dependence due to the effect of the size parameter X, the ratio of the particle perimeter to the wavelength of the incident radiation. The extinction coefficient of absorbing spheres are shown to be relatively uniform in X, unless they are in the Rayleigh scattering regime.[9] Such effects can also be seen for particles of other shapes. Even the nonabsorbing particles are relatively gray compared to the highly spectral gases. Although the particle nongray effects may still be significant, for the purposes of this study the particles are assumed to be gray, i.e., having properties that are independent of wave number. An additional source of spectral behavior is the nongray nature of the blackbody radiation, to which the layer emittance is compared.

The mixture properties are transformed to the equivalent nonscattering properties. The scaling laws for the mixture are given[4,5] as

1) Anisotropic to isotropic:

$$\kappa_i = (1 - \omega_a\langle\cos\theta\rangle)\kappa_a \tag{2a}$$

$$\omega_i = \frac{\omega_a(1-\langle\cos\theta\rangle)}{1-\omega_a\langle\cos\theta\rangle} \tag{2b}$$

2) Isotropic to nonscattering:
Linear

$$\kappa_E = (1-\omega_i)\kappa_i \tag{3a}$$

$$\rho_E = 1 - [2/(0.75\,\kappa_{Li}\omega_i + 2)] \tag{3b}$$

Square root

$$\kappa_E = \sqrt{1-\omega_i}\,\kappa_i \tag{4a}$$

$$\rho_E = 2/\omega_i\,(1-\sqrt{1-\omega_i}) - 1 \tag{4b}$$

The spectral dependence is implied for all the variables in Eqs. (2-4). The subscripts are a, the original anisotropic layer; i, the scaled isotropic layer; E, the equivalent nonscattering layer; and L, the total layer thickness. The asymmetry factor of the anisotropic scattering phase function is $\langle\cos\theta\rangle$, which is a weighted integral of the phase function.[10] It is an excellent single parameter representation of anisotropic phase functions. The linear and the square root scaling laws are the two possibilities for the second step in scaling. In general, linear scaling is appropriate for dominant scattering (high albedo) and small optical depth problems.[5]

For the linear scaling, the particle scattering effects are completely separated from the gaseous absorption effects. The $a_{E\nu}$ includes all the absorption for the layer, and ρ_E is a function

only of the scattering. The linear scaled equivalent properties are obtained from the component properties when Eq. (1) is substituted into the above scaling equations.

$$k_E = a_{E\nu} = a_p + a_{g\nu} \tag{5a}$$

$$\rho_E = 1 - \{2/[0.75\, L\sigma(1 - \langle\cos\theta\rangle) + 2]\} \tag{5b}$$

Since all the particle properties are assumed to be gray, the wall reflectivity is also gray. This separation of the gray and the nongray components is highly desirable from a computational viewpoint but really only makes sense in the linear scaling limit. Physically, the linear scaling applies to problems, where the radiative heat flux distributions across the layers are nearly constant, due either to the optically thin or the pure scattering limiting behavior. This implies that the relative positions of the scatterers within the medium cannot be a factor, and the problem could be modeled by putting all the scattering effects on the walls. Consequently, having the wall reflectivity include all the scattering effects is consistent with this scaling limit.

In the square root scaling regime, the component properties are impossible to sort out. It is also more difficult to understand the interactions between the particle and the gas properties. The square root scaled equivalent properties are obtained by combining the properties relationship of Eq. (1) with the scaling laws given in Eqs. (2) and (3):

$$a_{E\nu} = \sqrt{(a_p + a_{g\nu})^2 + (a_p + a_{g\nu})\sigma(1 - \langle\cos\theta\rangle)} \tag{6a}$$

$$\rho_{E\nu} = \frac{2 - \omega_a(1 + \langle\cos\theta\rangle) - 2\sqrt{(1 - \omega_a\langle\cos\theta\rangle)(1 - \omega_a)}}{\omega_a(1 - \langle\cos\theta\rangle)} \tag{6b}$$

where ω_a is the anisotropic scattering albedo given by Eq. (1b). Both $\rho_{E\nu}$ and $a_{E\nu}$ include the gas absorption and the scattering properties. Some type of nonlinear interaction between absorption and scattering within the medium does make sense, since the square root law is more accurate for the optically thick cases where multiple scattering effects dominate. The influence of the gas properties on the wall equivalent reflectivity is puzzling, since the function of the equivalent reflectivity is to model the backscattering from a layer. It should only be a function of the particle scattering characteristics.

A rigorous implementation of the square root scaling proved to be difficult because of the constraints of the exponential wideband gas model. The model yields information on the integrated band absorptance, instead of $a_{g\nu}$. The equivalent absorption coefficient given by Eq. (6a), which involves $a_{g\nu}$ and other function of gray particle properties, could not be related to the band absorptance. An approximate solution technique is therefore developed for the square root region. The scaled properties are taken to be

$$a_{E\nu} = a_{Ep} + a_{g\nu} \tag{7a}$$

$$\rho_E = \rho_{Ep} \tag{7b}$$

An approximate $a_{E\nu}$ is obtained by applying the square root scaling only to the particle properties—and then adding $a_{g\nu}$. This retains some of the nonlinear interactions between absorption and scattering evident in Eq. (6). The equivalent reflectivity is forced to be a function of the particle properties only, by square root scaling only the particle properties. The results presented later are obtained by using this approximate square root formulation in combination with the linear scaling.

Hemispherical Total Emittance

Scaling the mixture layer to an equivalent nonscattering layer is the beginning step in calculating the total hemispherical emittance. Through the scaling, an anisotropic scattering layer with cold, transparent boundaries is replaced by an absorbing-emitting layer with diffuse, reflecting walls. The emittance calculation is reduced to a problem of radiative heat flux exiting a gas-like layer, which is bounded by reflecting walls. A hemispherical emittance calculation involves an integration of all the paths through the planar slab as the energy exiting angle is varied. The integration over the wave numbers needed to obtain a total quantity is performed by dividing the spectrum into discrete intervals or bands. The wave number integral then becomes a sum over all the gas absorption bands given by the exponential wideband model. The windows between the band also need to be included in this analysis because the particle properties are assumed to be gray.

The system geometry and a schematic of the scaling discussed in the previous section are shown in Fig. 1. A slab of thickness L contains scattering particles and absorbing gases at a uniform temperature T. The component properties and the spatial coordinates are noted in the left figure, although the subscript a is deleted in the figure for clarity. The hemispherical total emittance of a layer is defined as

$$E_{p-g} = \frac{q^-(0)}{\sigma T^4} = \frac{\int_0^\infty q_\nu^-(0)\, d\nu}{\sigma T^4} \tag{8}$$

where $q^-(0)$ is the radiative heat flux in the negative y direction evaluated at the location $y = 0$. With the band approximation, the integral is replaced by a sum over all the bands.

The particle-gas layer is scaled to an equivalent nonscattering layer shown to the right in Fig. 1. Since the reflecting walls are imaginary and cannot contribute additional energy into the layer, T_w is set equal to 0 K. The radiative heat flux from the equivalent layer is given by the following equation:[6]

$$q_\nu^-(0) = \frac{-(1 - \rho_E)(1 - \langle\tau\rangle_\nu)}{1 - \rho_E\langle\tau\rangle_\nu} e_{bb,\nu}\, d\nu \tag{9}$$

where $e_{bb,\nu}$ is the spectral blackbody emissive power at the medium temperature, and $\langle\tau\rangle_\nu$ is the spectral geometric-mean transmittance given by

$$\langle\tau\rangle_\nu = \frac{1}{A_1 F_{1\text{-}2}} \int_{A_1}\int_{A_2} \frac{\tau_\nu(S)\cos\theta_1\cos\theta_2\, dA_1\, dA_2}{\pi S^2} \tag{10}$$

The $\langle\tau\rangle_\nu$ can be compared to the configuration factor for enclosures with nonparticipating media $F_{1\text{-}2}$, in which the transmittance along a path $\tau_\nu(S) = \exp(-a_{E\nu}S)$ is equal to 1. The effect of the absorbing medium and all the different paths needed to integrate over the hemisphere is included in $\langle\tau\rangle_\nu$. When the $\langle\tau\rangle_\nu$ is evaluated, the hemispherical part of the integration is complete.

The wave number integration for pure gas layers can be performed by two techniques when the exponential wideband model is used: the center and the block calculations.[7] The center calculation method is easier to apply than the block calculation, but it does not account for any possible overlap between the bands. The block procedure yields more accurate results, although it introduces a little more computational complexity. It is thus possible to define wave number integrated or averaged, geometric-mean transmittance for absorbing gases in

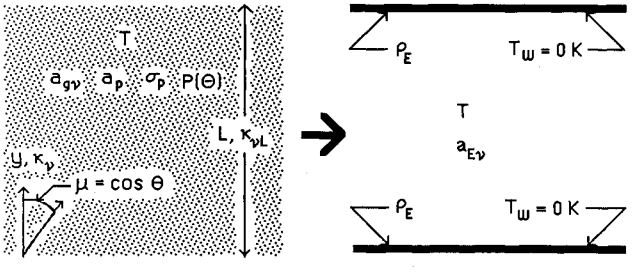

Fig. 1 System figure: particle-gas layer scaling.

terms of the integrated band absorptance A_j. When there is particle presence, which gives rise to a nonzero ρ_E, the integration of Eq. (9) in the strict sense no longer allows for a direct use of the band integrated gas quantities. To use the gas band model, the integration of Eq. (9) is approximated by a term by term integration. This approximation is expected to be accurate for small ρ_E limit and when the $\langle\tau\rangle_\nu$ is nearly a constant value and can be pulled out of wave number integration. The details of the center calculation with the approximate integration are given in the next subsection, followed by a description of the block calculation method.

Center Calculations

This method replaces all the medium spectral quantities with the band averaged values. The emissive power is then evaluated at the center of the band. After the term by term integration of Eq. (9), the total hemispherical emittance becomes

$$E_{p-g} = \sum_j \frac{-(1-\rho_E)(1-\langle\tau\rangle_j)}{1-\rho_E\langle\tau\rangle_j} \frac{e_{bb,j}\Delta\nu}{\sigma T^4} \tag{11}$$

The sum is over the bands, and the quantities with the subscript j are band averaged. The ρ_E is assumed to be a constant value for both the linear and the approximate square root scaling laws. The $\Delta\nu$ is the band width, which is set equal to the exponential band decay width ω_b. The e_{bb} is given by the Planck function multiplied by π. Since the $e_{bb,j}$ is calculated at the band center, this formulation is called the center calculation.

Evaluating the $\langle\tau\rangle_j$ is the key step in the solution procedure, since all the information concerning the nongray gas and gray particle interactions are contained in it. Equation (10) for $\langle\tau\rangle_\nu$ is greatly simplified for a plane parallel layer, although a double integration over the path lengths and the wave number is still required. The gas transmittance is expressed in terms of A_j^*, and the integral over the path lengths is transformed to an integral over μ from 0 to 1:

$$\langle\tau\rangle_j = 2E_3(a_{Ep}D) - \int_0^1 \exp\left(\frac{-a_pD}{\mu}\right) A_j^*\left(\frac{\tau_H}{\mu},\eta_b\right) 2\mu\, d\mu \tag{12}$$

where E_3 is the third-order exponential integral function. This integration is carried out numerically, using a Gaussian quadrature of order forty. At each quadrature point, A_j^* is reevaluated as τ_H/μ changes.

In the windows between the gas bands, $\langle\tau\rangle_\nu$ is gray and can be analytically evaluated to be equal to $2E_3(\kappa_{LE,p})$. The $\kappa_{LE,p}$ is the total equivalent optical depth obtained by considering just the particle properties. Since the particle emission is a constant, the center calculation is modified in the window regions. Instead of evaluating $e_{bb,j}$ at the center, $f(\nu_u T) - f(\nu_l T)$, the difference in the blackbody fractions at the band limits, is used for better accuracy in the window regions.

Block Calculations

This method uses band averaged quantities that are different than those for the center method, and it also uses $f(\nu T)$ instead of e_{bb}. The block calculation method has been shown to be more accurate than the center calculation for gases that have overlapping bands. The accuracy is also better for such gases as H_2O, which has a wide rotational band. Block calculation procedure for gases begins with finding the band absorption A_j. A band transmittance is then assigned as

$$\tau_{b,j} = \left(\frac{\tau_{Hj}}{A_j^*}\right)\left(\frac{dA_j^*}{d\tau_{Hj}}\right) \le 0.90 \tag{13}$$

The width of the band is established as

$$\Delta\nu_j = \nu_{u,j} - \nu_{l,j} = [A_j/(1-\tau_{b,j})] \tag{14}$$

When there is an overlap between the adjacent bands, a new band is formed, which has $\tau_{b,j}$ equal to the multiple of the two original band transmittances. Transparent windows are assigned $\tau_{b,j} = 1.0$. Bands are than "blocked" off and sorted to cover the entire spectrum.

The effect of the particles are included for each blocked band, by multiplying $\tau_{b,j}$ with the $\tau_p = \exp(-a_{Ep}S)$. The $\langle\tau\rangle_\nu$ can then be calculated as a function of the particle and gas transmittances. When the approximate integration of Eq. (9) becomes a sum of the integrals over the bands, all of the leading terms are constant. Only $e_{bb,\nu}$ remains in the integral. Dividing through by σT^4 to obtain E_{p-g} allows for the evaluation of the integral as $f(\nu_u T) - f(\nu_l T)$.

The blocking described thus far is easily implemented for any path length S through the layer. It is during a hemispherical calculation that the difficulties arise. As all exiting angles are considered, the path lengths through the medium change, resulting in changes in $\tau_{H,j}$. This influences A_j^* directly, according to the band correlation used. A different A_j^* results in not only a different $\tau_{b,j}$ but also in different band limits [see Eq. (14)]. The band limits dictate the blackbody fractions that must be evaluated. There is then a direct coupling between the spectral and the hemispherical integrations, which are independently handled for the center calculations.

The approach of this work is to compute the full block calculation at each length τ_H. For each wave number integrand of Eq. (9), which involves the hemispheric integration over μ, the order of integration is switched. The effect is to define a wave number averaged, or total, geometric-mean transmittance $\langle\tau\rangle$ and a total geometric mean absorptance $\langle\alpha\rangle$.

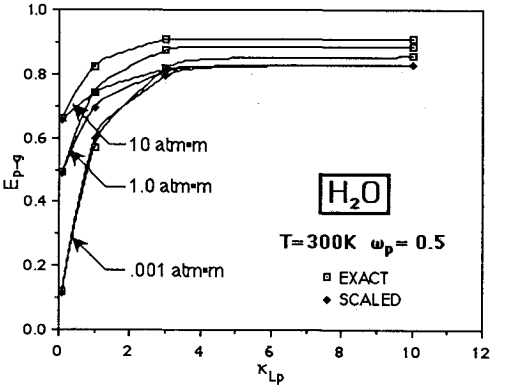

Fig. 2 Comparisons for H_2O: (T = 300 K, ω_p = 0.5, block calculation).

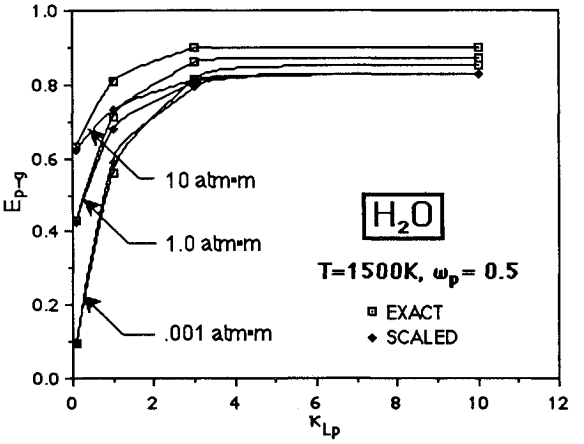

Fig. 3 Comparisons for H_2O: (T = 1500 K, ω_p = 0.5, block calculation).

$$\langle\tau\rangle = \int_0^1 \sum_j \tau_{bj} \exp\left(\frac{-a_{Ep}L}{\mu}\right)\{f(\nu_u T) - f(\nu_l T)\}\, 2\mu\, d\mu \quad (15a)$$

$$\langle\alpha\rangle = \int_0^1 \sum_j \left\{1 - \tau_{bj} \exp\left(\frac{-a_{Ep}L}{\mu}\right)\right\} \times \{f(\nu_u T) - f(\nu_l T)\}\, 2\mu\, d\mu \quad (15b)$$

The average geometric-mean transmittance and absorptance are then substituted into the integration result of Eq. (9). The hemispherical total emittance is then given by

$$E_{p-g} = \frac{-(1-\rho_E)\langle\alpha\rangle}{1-\rho_E\langle\tau\rangle} \quad (16)$$

The numerical scheme used for the center calculation is also used for the block calculation.

Results and Discussion

Calculations have been performed for suspensions of isotropic scattering particles in either H_2O or CO_2 gas. The total gas pressure is 1 atm and the partial pressure of the absorbing species P_a is taken toward the limiting value of zero. Layer temperature of 300 or 1500 K is considered. The optical thickness of the gaseous component is varied by taking P_aL, the product of the partial pressure and thickness, as 0.001, 1, and 10.0 atm · m. The particle optical depths of 0.1, 1.0, 3.0, and 10.0 are considered, and the scattering albedo is varied from 0.1 to pure scattering ($\omega_p = 1.0$). A sample of the results is presented here for discussion.

Comparisons between the exact and the scaled E_{p-g} are presented in Figs. 2-7. The cases represent $\omega_p = (0.1, 0.5)$ and $T = (300\text{ K}, 1500\text{ K})$. Water vapor is the absorbing gas in Figs. 2-5 ($P_aL = 0.001, 1.0, 10$ atm · m), and carbon dioxide is the absorbing gas in the Figs. 6 and 7 ($P_aL = 0.001, 10$ atm · m). The comparisons when the particles approach the pure scattering limit ($\omega_p = 0.95, 1.0$) are presented in Tables 1 and 2. The scaled calculations have been performed using both the block and the center calculation procedures. All of the presented results use a combination of linear and square root scaling, depending on the scaling regimes given in Ref. 5. The square root scaling follows the approximate scaling technique described in the scaling properties section. The exact results[8] are based on the photon path length distribution method, which

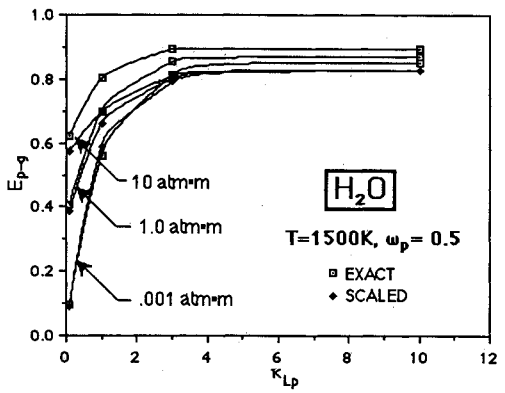

Fig. 4 Comparisons for H_2O: (T = 1500 K, ω_p = 0.5, center calculation).

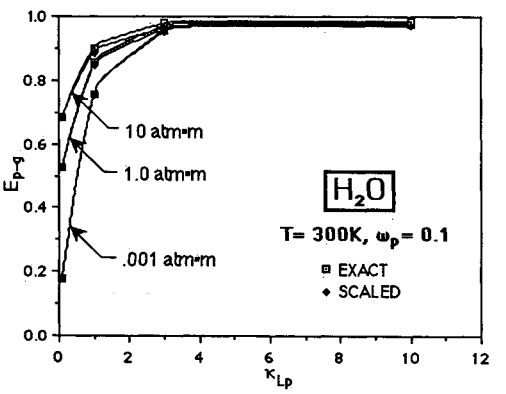

Fig. 5 Comparisons for H_2O: (T = 300 K, ω_p = 0.1, block calculation).

Table 1 Comparisons for H_2O and CO_2: (ω_p = 0.95, κ_{Lp} = 1.0)

H_2O block calculations

P_aL	E_{p-g} (exact)	E_{p-g} (scaled)	% error
	T = 300 K		
0.001	0.1224	0.1124	−8.16
1	0.4873	0.4196	−13.8
10	0.6541	0.5357	−18.1
	T = 1500 K		
0.001	0.0994	0.0907	−8.75
1	0.4232	0.3732	−11.8
10	0.6208	0.5147	−17.0

CO_2 block calculations

P_aL	E_{p-g} (exact)	E_{p-g} (scaled)	% error
	T = 300 K		
0.001	0.1126	0.1033	−8.25
1	0.2438	0.2227	−8.65
10	0.3018	0.2715	−10.0
	T = 1500 K		
0.001	0.1073	0.0983	−8.38
1	0.2608	0.2376	−8.89
10	0.3564	0.3175	−10.9

Table 2 Comparisons for H_2O and CO_2: (ω_p = 1.0, κ_{Lp} = 3.0)

H_2O block calculations

P_aL	E_{p-g} (exact)	E_{p-g} (scaled)	% error	E_g
		T = 300 K		
0.001	0.0293	0.0296	1.02	0.0306
1	0.4164	0.2970	−28.6	0.4460
10	0.5995	0.3691	−38.4	0.6313
		T = 1500 K		
0.001	0.0043	0.0042	−2.32	0.0042
1	0.3428	0.2649	−22.7	0.3773
10	0.5592	0.3571	−36.1	0.5968

CO_2 block calculations

P_aL	E_{p-g} (exact)	E_{p-g} (scaled)	% error	E_g
		T = 300 K		
0.001	0.0181	0.0190	4.97	0.0194
1	0.1585	0.1411	−10.9	0.1677
10	0.2225	0.1843	−17.1	0.2325
		T = 1500 K		
0.001	0.0124	0.0131	5.64	0.0133
1	0.1758	0.1551	−11.7	0.1879
10	0.2780	0.2221	−20.1	0.2960

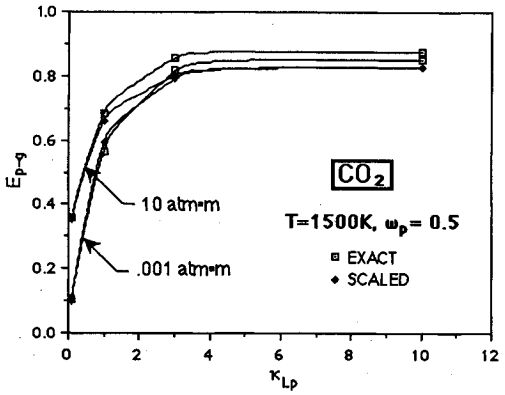

Fig. 6 Comparisons for CO_2: (T = 1500 K, ω_p = 0.5, block calculation).

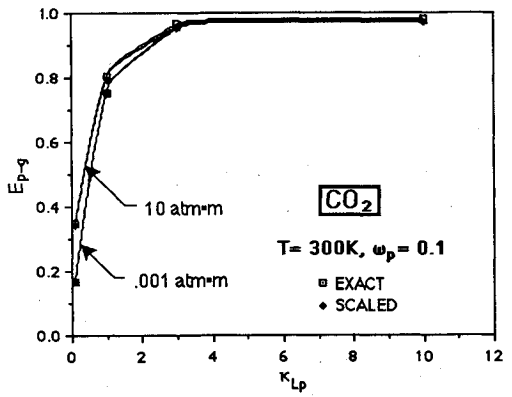

Fig. 7 Comparisons for CO_2: (T = 300 K, ω_p = 0.1, center calculation).

includes the hemispherical gas absorption, rather than a mean beam length for the gas absorption.

A discussion of the center vs the block calculation procedure is presented first. The accuracy of the scaled solution with the changing problem parameters is then discussed. The following effects are considered: ω_p (change in the composition of the particles), κ_{Lp} (change in the number concentration of the particles), and P_aL (change in the absorbing gas concentration). The accuracy of the equivalent E_{p-g} is found not to depend on the temperature of the mixture, i.e., there is very little difference between the results shown in Fig. 2 at 300 K and the results for the same albedo at 1500 K shown in Fig. 3. The albedo effect dominates, as compared to the temperature effect.

The differences between the block and center calculations have already been noted for gases.[2] Same kinds of trends are also noted when the scaled solutions are compared, e.g., there can be an appreciable difference for H_2O mixtures of low temperature but not for CO_2 mixtures. A direct comparison between the two methods is shown in Figs. 3 and 4 for H_2O-particle mixtures. Since the temperature is high, there is no difference between the exact results as there is when the temperature is lower, T = 300 K. The figures do show what is important for this work, namely, even when the exact solutions are similar, the scaled solution accuracy is better if the block procedure is used. Although the figures are not shown, this conclusion is also valid for CO_2. This difference in the scaling accuracy between the block and the center calculation is very pronounced for large P_aL and ω_p at the low κ_{Lp} limit. The differences get washed out as κ_{Lp} approaches the optically thick limit. In the figures that follow, the center results are given only when the accuracy is comparable to the block results. The trends that are discussed below hold true for both the center and block calculations.

Figures 5 and 7 show the excellent accuracy of the scaled solution for small albedo problems, regardless of the particle loading (κ_{Lp}), P_aL, or the gas species. When ω_p is small, particle behavior resembles that of the gases, i.e., mostly absorbing and emitting. Since the scaled layer only absorbs and emits, it is naturally a very accurate model for this limit. The ω_p = 0.5 figures (Figs. 2-4 and 6) illustrate the effect of the increasingly strong scatterers. Notice the good accuracy in the equivalent solution for small P_aL and κ_{Lp}, but the discrepancy between the exact and the scaled solution increases as κ_{Lp} and P_aL increases.

Some of the results for the dominant scattering problems (ω_p = 0.95, κ_{Lp} = 1.0) are shown in Table 1. The results for ω_p = 1.0 and κ_{Lp} = 3.0 cases are presented in Table 2. The tables present the exact and the scaled emittances as well as the percent difference for different T's and P_aL's. The results presented in Table 1 have been compared with those for ω_p = 0.5 (see Figs. 2-4 and 6). The difference in accuracy between the ω_p = 0.5 and 0.95 is roughly a factor of two in percent difference. The increase in the scattering albedo aggravates the inaccuracy for high P_aL, also shown in Figs. 2-4 and 6. Results shown in Table 2 represent the severest test case with the worst accuracy. The only exception to note is the small P_aL limit, where the scaled solution is still very accurate.

The pure scattering problem is special in that the particles only redirect the incident energy, i.e., there is no emission or absorption by the particles. The only contribution to the layer emittance must be from the gas. Yet comparing the pure gas hemispherical emittance E_g, also presented in Table 2, to the mixture E_{p-g} shows an influence of the particles. The scaling, which is linear in these cases, separates the particle and the gas effects. The increased scattering results in higher ρ_E, which reduces the scaled emittance. The presence of highly scattering particles reduces the effectiveness of the gas emission, since the particles multiply scatter the emitted radiation and make it more difficult for the energy to exit the layer.

In all the figures and the tables, the accuracy of the scaled solution is shown to be excellent when κ_{Lp} is very small for all ω_p and P_aL. These cases correspond to problems that are mostly gas problems, and the scaling correction is small. The increase in the accuracy with the block calculation is most profound for the small κ_{Lp}. As the κ_{Lp} increases, the scaling law switches over to the square root for all the cases except for the dominant scattering problems. As the solutions reach an optically thick limit at κ_{Lp} of roughly four, the error in the scaling also approaches a steady value.

The limitation of the approximate square root scaling becomes evident toward the optically thick limit. Because the square root scaling is applied only to the particles, the scaled solution does follow trends similar to the exact solution as κ_{Lp} increases. The real failure for the approximation is in the P_aL effect. The overall solution accuracy, except for the low albedo cases, is noticeably worse for larger P_aL. The scaled solution also approaches the thick limit independent of P_aL. The accuracy could be improved if $a_{g\nu}$ were better incorporated into the square root scaling.

An aggravating factor for the P_aL error is the way in which the scaling law regimes were determined. Strictly speaking, the mixture κ_a and ω_a need to be considered at each ν to decide on the scaling. Since the information on $a_{g\nu}$ is not available, only the gray particle properties were considered. In the transition between the two scaling laws, some inaccuracy may thus be introduced. The gas absorption increases κ_a and may push a linear problem to the square root scaling. This error is small when P_aL or ω_p is small but can be large at high P_aL. For the dominant scattering problems, the scaling is definitely linear in the windows of the gas absorption, but at various ν's within the absorbing bands, γ may be large enough to put ω_a in the square root range. Since it is impossible to do the scaling at every ν, scaling for each gas band could be considered. A band-averaged a_{gj} then needs to be obtained, possibly with a method similar to that used in Ref. 11.

The overall solution accuracy is also affected by the approx-

imation made in the spectral integration of Eq. (9). The numerator and the denominator are integrated separately, which is not a permissible operation. This approximation has been made to obtain Eqs. (11) and (16), which directly use the integrated gas band properties. The approximation can only be accurate in the limit of the denominator going to one, i.e., ρ_E going to zero. The approximation is also valid if the spectral dependence of $\langle\tau\rangle_\nu$ is minimal and can be considered to be a constant value, i.e., valid at the very low gas concentrations given by low P_aL values.

The solution accuracy is seen to be excellent for the low P_aL values regardless of the particle concentration or properties. The accuracy is also excellent for the optically thin limit, even when the albedo is high, because the resulting equivalent reflectivity is very small. The accuracy is considerably worse for high P_aL and ρ_E values. The effect of the integration error is further compounded by the error in the square root scaling approximation. A preliminary study indicates that the dominant error is from the scaling approximation. Improvements in the square root scaling and a determination of the optical depth, including the gas component at each band, is where the future effort needs to be directed.

Conclusions

A solution method is developed to obtain the hemispherical emittance of isothermal layers composed of absorbing gas and scattering particles. Previously developed scaling laws transform the mixture properties to equivalent nonscattering properties. The linear scaling is simple to apply and understand. An approximate square root scaling has been introduced, which is easy to use, but is shown to have only limited accuracy. Hemispherical calculation procedure is developed using both the center and the block calculation methods. Although the center method is easier to apply, the block calculations result in more accurate results. Absorbing gases of H_2O and CO_2, together with isotropically scattering particles, are considered. The scaled equivalent results are compared to calculations available from the path length distribution solution. Excellent comparisons are obtained for low to moderate absorbing gas pressures and for low to moderate particle optical depths and albedos. The scaled solution is also good for all κ_{Lp}, if P_aL and ω_p are not large. Some improvement in the accuracy of the scaled solution could result if the scaling law regime was determined at each gas band. Significant improvement in the accuracy requires a better formulation of the square root scaling.

Acknowledgments

This work was supported in part by the National Science Foundation Grant NSF/CBT-8451076. This PYI award was also supported by the McDonnell Douglas Foundation. Thanks to D.V. Walters for doing the path length distribution calculations. Special thanks are extended to Dr. Richard Buckius for his generous sharing of ideas and support.

References

[1]Bakan, S., Koepke, P., and Quenzel, H., "Radiation Calculations in Absorption Bands: Comparisons of Exponential Series- and Path Length Distribution-Method," *Contributions of Atmospheric Physics,* Vol. 51, 1978, pp. 28–30.

[2]Skocypec, R. D. and Buckius, R. O., "Total Hemispherical Emittances for CO_2 or H_2O Including Particulate Scattering," *International Journal of Heat and Mass Transfer,* Vol. 27, No. 1, 1984, pp. 1–13.

[3]Yamamoto, G., Tanaka, M., and Asano, S., "Radiative Transfer in Water Clouds in the Infrared Region," *Journal of the Atmospheric Sciences,* Vol. 27, March 1970, pp. 282–292.

[4]Lee, H. and Buckius, R. O., "Scaling Anisotropic Scattering in Radiation Heat Transfer for a Planar Medium," *Journal of Heat Transfer,* Vol. 104, Feb. 1982, pp. 68–75.

[5]Lee, H. and Buckius, R. O., "Reducing Scattering to Nonscattering Problems in Radiation Heat Transfer," *International Journal of Heat and Mass Transfer,* Vol. 26, No. 7, 1983, pp. 1055–1062.

[6]Siegel, R. and Howell, J. R., *Thermal Radiation Heat Transfer,* 2nd ed., Hemisphere, Washington, DC, 1981.

[7]Edwards, D. K., "Molecular Gas Band Radiation," *Advances in Heat Transfer,* Vol. 12, 1976, pp. 115–193.

[8]Skocypec, R. D., Walters, D. V., and Buckius, R. O., "Total Hemispherical Emittances for Isothermal Mixtures of Combustion Gases and Scattering Particulate," *Combustion Science and Technology,* Vol. 47, 1986, pp. 239–252.

[9]van de Hulst, H. C., *Light Scattering by Small Particles,* Dover, 1957.

[10]Irvine, W. M., "The Asymmetry of the Scattering Diagram of a Spherical Particle," *Bulletin of Astronomical Institute of the Netherlands,* Vol. 17, No. 3, 1963, pp. 176–184.

[11]Menguc, M. P. and Viskanta, R., "An Assessment of Spectral Radiative Heat Transfer Predictions for a Pulverized Coal-Fired Furnace," *Proceedings of the 8th International Heat Transfer Conference,* Vol. 2, Hemisphere, Washington, DC, 1986, pp. 815–820.